Laboratory Investigation (2004) 84, 1404–1417

www.laboratoryinvestigation.org

Epithelium–mesenchyme compartment interaction and oncosis on chemotherapy-induced hair damage

Silvia Selleri[1], Francesca Arnaboldi[1], Laura Vizzotto[1], Andrea Balsari[2] and Cristiano Rumio[1]

[1]*Department of Human Morphology, Università degli Studi di Milano, Milano, Italy and* [2]*Institute of Pathology, National Cancer Institute, Università degli Studi di Milano, Milano, Italy*

It is known that chemotherapy induces alopecia in humans, with important psychological and social implications in spite of its reversibility. Among chemotherapeutic drugs, anthracyclines are widely used, yet cause severe alopecia. One of the causes for the elevated sensibility of hair follicles to anthracyclines, and to drugs in general, is the high proliferation rate of follicular epithelium and the long duration of the growth phase (up to 7 years in humans). To clarify the mechanism of anthracycline toxicity, we used a rat model and focused our attention on the morphological alterations in hair follicles induced by doxorubicin. We observed the progression of hair follicle degeneration in the epithelial and mesenchymal compartments until alopecia arose, by both light and electron microscopy. As a first sign of damage, significant apoptosis was detected in the proximal perifollicular connective tissue sheath and sporadically in the matrix, near the interface between matrix and follicular papilla. We propose the apoptotic remodeling of the mesenchymal compartment as a process that is fundamental to the progression of events leading to alopecia. Regarding the epithelial compartment, it is important to note that oncosis was observed in a large number of follicular cells in the outer root sheath during the last stages of hair follicle regression. This indicates that oncosis is involved in a major way in the damage of epithelial cells.
Laboratory Investigation (2004) **84,** 1404–1417, advance online publication, 20 September 2004; doi:10.1038/labinvest.3700170

Keywords: alopecia; chemotherapy; hair follicle; oncosis; doxorubicin

Damage of hair follicles (HF) and subsequent hair loss is a common side effect of the administration of cancer chemotherapeutic drugs in humans.[1] The severity of alopecia is drug, dose and schedule dependent.[2] Among chemotherapeutic drugs, anthracyclines are widely used but cause severe alopecia in up to 80% of cancer therapy cases.[3] The high toxicity of anthracyclines and chemotherapeutic drugs in general, to follicles depends on the high proliferation rate of the cells composing their structure. Moreover, HFs are miniorgans that are supplied by a rich blood flow, thus rendering HFs a privileged site for the accumulation of many compounds.[4]

Alopecia is commonly reversible, but poses a problem from a psychological point of view due to the association of hair loss with the loss of attractiveness, individuality, changes in self-concept and body image.[5] In addition, patients can suffer evident alterations in hair color and texture[6] upon subsequent hair growth. These psychosocial implications may lead to the refusal of treatment,[7] hence outlining the interest in studies aimed at the prevention of alopecia.

Although many studies aimed at understanding the phenomena that drives hair follicle degeneration after chemotherapy have been performed to date, effective methods preventing hair loss are still lacking. Several studies using animal models, in which alopecia was induced by drug treatment, suggested that alopecia induced by chemotherapeutics is principally mediated by the induction of apoptosis within the proliferative-epithelial compartment.[8,9] On the other hand, a study performed with morphological methods, indicated that apoptosis within the epithelial compartment is present in a low percentage of cells after treatment.[10] These preliminary statements lead us to further study the modality of cell death or degeneration that

Correspondence: Professor C Rumio, Department of Human Morphology, Università degli Studi di Milano, Via Mangiagalli, 31, Milano 20133, Italy.
E-mail: cristiano.rumio@unimi.it
Received 31 May 2004; revised and accepted 8 July 2004; published online 20 September 2004

cooperates with apoptosis to drive HF degeneration. Recent careful morphological observations by Tobin *et al*[11] have underlined as HF is a refined miniorgan, in which cycling life depends on a complex series of interactions between epithelial and mesenchymal compartments.

On these bases, we investigated the effects of chemotherapy on both epithelium and mesenchyme from a morphological point of view using a rat model previously described by Hussein *et al*.[12] We focused particular attention to the different steps occurring from the first signs of HF suffering to the arise of alopecia.

We observed that both structural and ultrastructural morphological modifications affected the epithelial and mesenchymal compartments of the HF and that besides apoptosis, oncosis was involved in hair follicle degeneration. Oncosis (from '*ονκος*', meaning swelling) is defined as a form of cell death characterized by cellular and organelle swelling and increased membrane permeability.[13] The mechanism of oncosis is due to the failure of the ionic pumps localized on the plasma membrane, generally caused by ischemia or toxic agents that increase membrane permeability. Data reported in literature suggest that this process can be involved in cell death induced by oxidative stress[14] and in particular in cells treated with doxorubicin (DXR).[15] From a molecular point of view, Mills *et al*[16] recently proposed that the expression of uncoupling protein 2 (UCP2) can induce oncosis, while its inhibition can selectively protect cells from oncotic stress but not from apoptosis. This indicated that oncosis is a cell death phenomenon that can be theoretically targeted, even though it is not yet fully understood.

Our findings regarding the mechanism of chemotherapy-induced cell death may be useful in future studies aimed at preventing hair loss.

Matherials and methods

Animals

For the animal model of chemotherapeutic-induced alopecia, we referred to the method of Hussein *et al*,[12] with minor modifications: 7-day-old rats, with hair follicles in the first postnatal anagen phase, were intraperitoneally injected with DXR 3 mg/kg/day for 4 days. Mild or severe alopecia (at least 50 or 80% respectively of the total occipital region, personal observation) arose suddenly around 10 days after the first injection (17 days p.n.), in the head and proximal neck regions in nearly 80% of injected rats. In total, 90 animals were treated and 14 animals were used as negative controls. Samples of skin were taken from rats (four treated and one control) that were killed daily during DXR treatment and for a period of time after treatment, until alopecia arose. Skin samples were collected from the affected area and processed for histological and ultrastructural analyses.

Animal studies have been performed in accordance with the guidelines of the Human Morphology Department on the use of laboratory animals.

Histological and Ultrastructural Analysis

Representative skin tissue samples from DXR treated and control rats (2×4 mm) were fixed in 3% glutaraldehyde in 0.1 M phosphate buffer (pH 7.4) for 3 h at 4°C, washed in 0.1 M phosphate buffer and postfixed in 1% osmium tetroxide (OsO_4) in 0.1 M phosphate buffer. Samples were dehydrated through an ascending series of ethanol and embedded in Araldite. Ultrathin sections 70 nm thick) were cut on a diamond knife, with a Reichter Ultracut R ultramicrotome (Leica, Wien, Austria) and stained with uranyl acetate and lead citrate. Samples were observed with a Jeol CX100 transmission electron microscope (Jeol, Tokyo, Japan). Semithin sections 700 nm thick) were stained with toluidine blue for observations with a Nikon Eclipse 600 (Nikon, Tokyo, Japan) light microscope and the images were collected with a digital camera (Nikon DXM1200).

For statistical analysis of the incidence of oncosis, mitosis and apoptosis, we collected data from two treated animals and one control for each of the time points. At least 50 hair follicles from each animal were considered. Each follicle was divided into three compartments: proximal connective tissue sheath (CTS), matrix (keratinocytes under Auber's line)[17] and outer root sheet (ORS). Data regarding the cells of the epidermis were obtained from at least eight nonserial sections derived from two different blocks per animal.

Light Microscopy Morphometric Analysis to Recognize Oncotic Cells

We identified oncotic cells according their morphological features: a large round-shaped nucleus with an evident nucleolus and a cytoplasm showing poor affinity to toluidine blue.

To confirm our opening observations, we have measured the section area of about 250 nuclei of normal and oncotic cells, from digital images of semithin sections acquired with a $\times 40$ oil objective. Nuclei were manually outlined and areas measured with the image analyzer program LaserPix (version 4.0, BioRad), after an appropriate calibration. The mean values were 17.92 μm^2 in normal cells and 89.28 μm^2 in oncotic cells (t-test = 25.63, $P < 0.001$). If profiles are considered circular, these values correspond to a section diameter of about 4.7 and 10.7 μm. However, the nuclei of normal cells are usually elongated, while they tend to be rounded in oncotic cells; irrespectively though, the difference in area is quite obvious.

Alkaline Phosphatase Staining to Detect FP Cells

Samples of skin were submerged in liquid N_2 vapors and subsequently included in OCT. Cryostatic sections of 7 μm were obtained and stored at -30°C until used.

Specific staining was performed on cryostatic sections using the BCIP/NBT liquid substrate system (Sigma-Aldrich, St Louis, MO, USA), according to the manufacturer's instructions. Briefly, sections were dried at room temperature (RT), fixed with cold acetone (-30°C) for 3 min, washed with physiological solution (0.9% NaCl in bidistilled water), incubated with the reagent (1–2 min) at RT in the dark, washed with bidistilled water and mounted with Mowiol (Calbiochem, Merck, Darmstadt, Germany).

Statistical Analysis

At the different time points, apoptotic, mitotic and oncotic cells were counted. Mean percentages and relevant standard errors are quoted. All data were subjected to univariate variance analysis, using a fully factorial model. In all the significant cases,[18,19] a *post hoc* Scheffé test was carried out (SPSS-version: Windows 11.5.1).

Results

Here we present results referring to the four time points that best represented the general dynamics of the observed process. Between closer times points, no appreciable differences were evident. The outline of the experiment is reported in Figure 1. Treated animals received the first DXR dose at time T0 and therefore, T1 indicates animals that received one dose and were killed 24 h later, T5 indicates animals that received all four doses and were killed 24 h later. In the case of T7 and T10, animals were sacrificed respectively 3 and 6 days after the last DXR injection. In general, we observed a sudden degeneration of the entire hair follicle, beginning at T5 and proceeding to T7. By T10, the processes reached their maximum in which at least 50% of the head and 80% of the proximal neck skin surface showed alopecia. The time points mentioned above were thus selected because they best represented the dynamics of this observation.

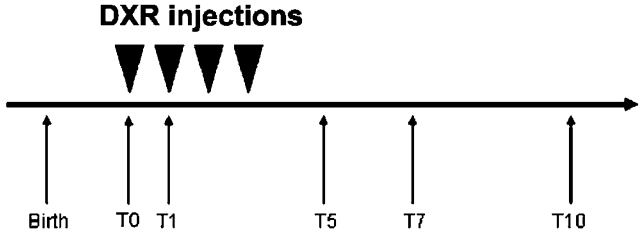

Figure 1 Outline of the experiment. Time points considered in the paper are indicated.

During the course of the experiment, we also noted that treated rats progressively lost weight and became smaller in size with respect to their untreated (control) littermates. The modifications occurring within the hair follicles at the different time points considered have been detailed below.

T1: HF and Epidermis do not Show Degenerative Features

Examination by light microscopy showed the four epidermal layers: basal, spinous, granular and cornified layers in the occipital region of T1. Basal layer cells faced the lateral sides and were prismatic in shape. In every layer of stratum granulosum, keratohyalin granules increased in size towards the stratum corneum. The stratum corneum, as seen in normal epidermis, included a variable number of layers containing corneocytes anucleated (Figure 2a).

HFs were in the anagen phase and were well organized in all portions of their complex architecture: inner root sheath (IRS), ORS, cuticles, cortex and medulla (Figure 3). Bulbs were big and included several cells that displayed a mitotic figure. Bulbs were placed within the panniculum adiposum and embraced the follicular papilla (FP) (Figure 4a, b).

Electron microscopy further confirmed the data regarding keratinocytes of the epidermis: keratohyalin granules were well defined in the stratum granulosum and cells showed elongated nuclei that generally followed cell shape as seen in normal epidermis. Cells of the basal and suprabasal layers were linked by numerous desmosomes and showed many mitochondria with well organized cristae (Figure 5e) and large keratin bundles (Figure 5a).

Within the hair follicle, ORS cells were large and clearly showed the presence of both glycogen granules and organelles such as the mitochondria and the endoplasmic reticulum within their cytoplasm (Figure 6a).

T5: Oncosis in the Epidermis—Apopotosis in the Matrix and in the CTS

At this time point, untreated animals did not show evident changes with respect to T1 by either light or electron microscopy. The follicles, however, as obviously expected, were in a more advanced stage of the anagen phase.

In the epidermis of treated animals, 18,6% of keratinocytes were oncotic (Tables 1 and 2; Figures 7a and 8). Under light microscopy, cells with enlarged nuclei with respect to the control were evaluated as oncotic. Morphometric analysis revealed that the surface area of oncotic nuclei was about five times greater than that of normal nuclei. Granules of the stratum granulosum appeared irregular in shape within the single cell layers and showed an abnormal coalescence, resulting in a

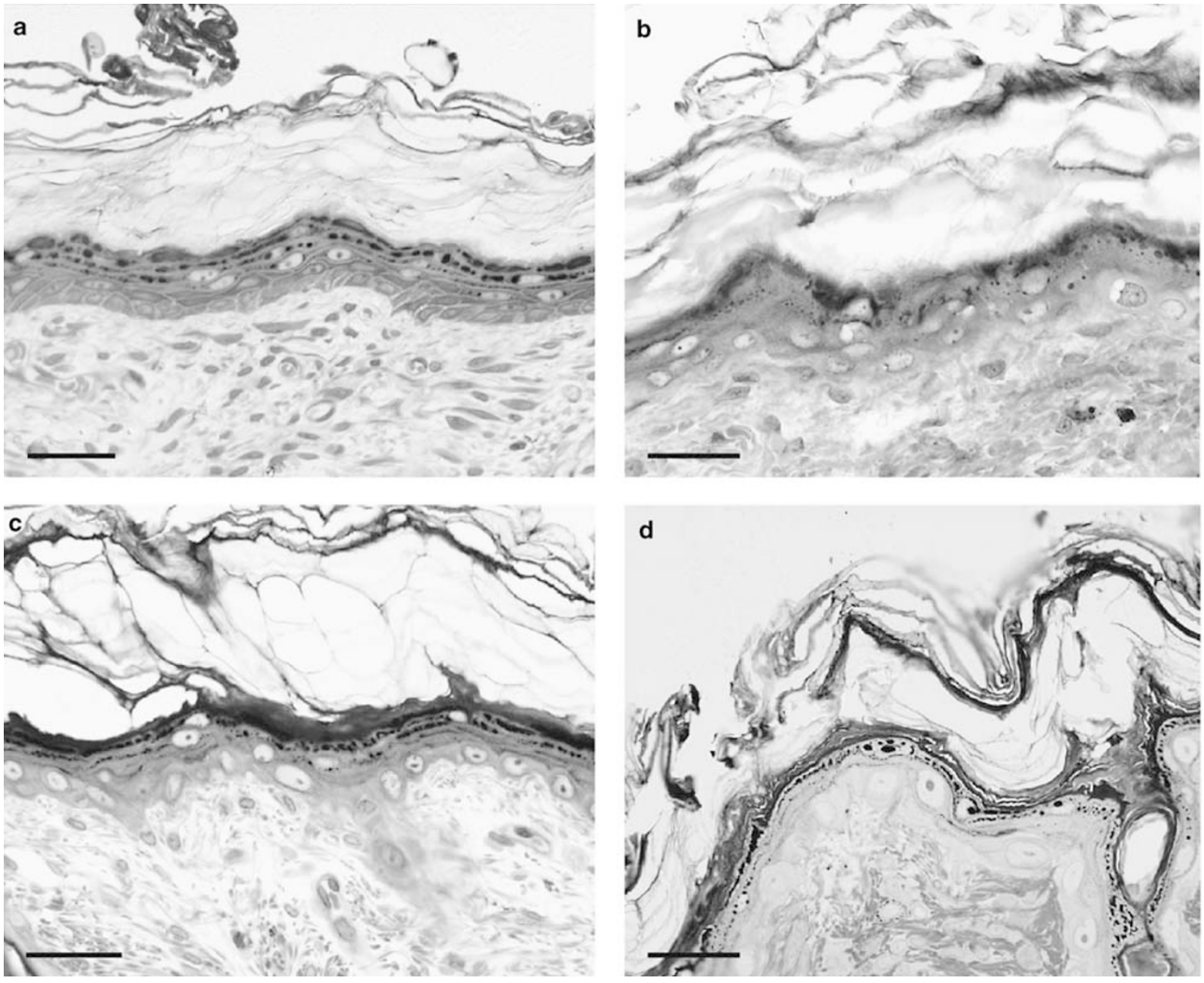

Figure 2 Semithin sections showing epidermis of treated rats at different time points. (**a**) T1; (**b**) T5; (**c**) T7; (**d**) T10. Note the progressive swelling of keratinocytes. Bar: 30 μm.

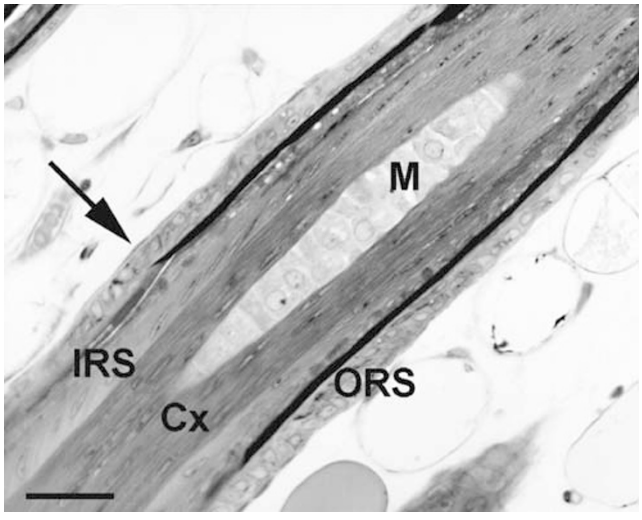

Figure 3 Semithin sections showing the structure of a normally organized HF at T1. Black arrow: CTS; M: medulla; Cx: cortex. Bar: 30 μm.

thick layer of cells that was intensely stained with toluidine blue (Figure 2b).

Hair follicles preserved their shape and mitotic forms were observed in the matrix (Figure 4c). At this time point, apoptotic figures were frequently observed in the proximal region of CTS (20.1% of the CTS fibroblasts) (Figure 4c; Tables 1 and 2; Figures 7d and 9) and sporadically within cells of the matrix (3.1% of matrix keratinocytes) near the interface between matrix and FP (Figure 4c, d; Tables 1 and 2; Figures 7c and 9). Apoptotic nuclei were not visible in either control or T1 samples. Fibroblasts of the FP began to assume an irregular shape, suggesting the shift to a quiescence state that became more evident in successive time points with the clustering of FP fibroblasts. Cell morphology and orientation appeared to divert from the typical organization of anagen V/VI, in which cells typically showed spindle-shaped nuclei with the major axis oriented parallel to the direction hair growth (Figure 4c). As was observed in the epidermis, ORS

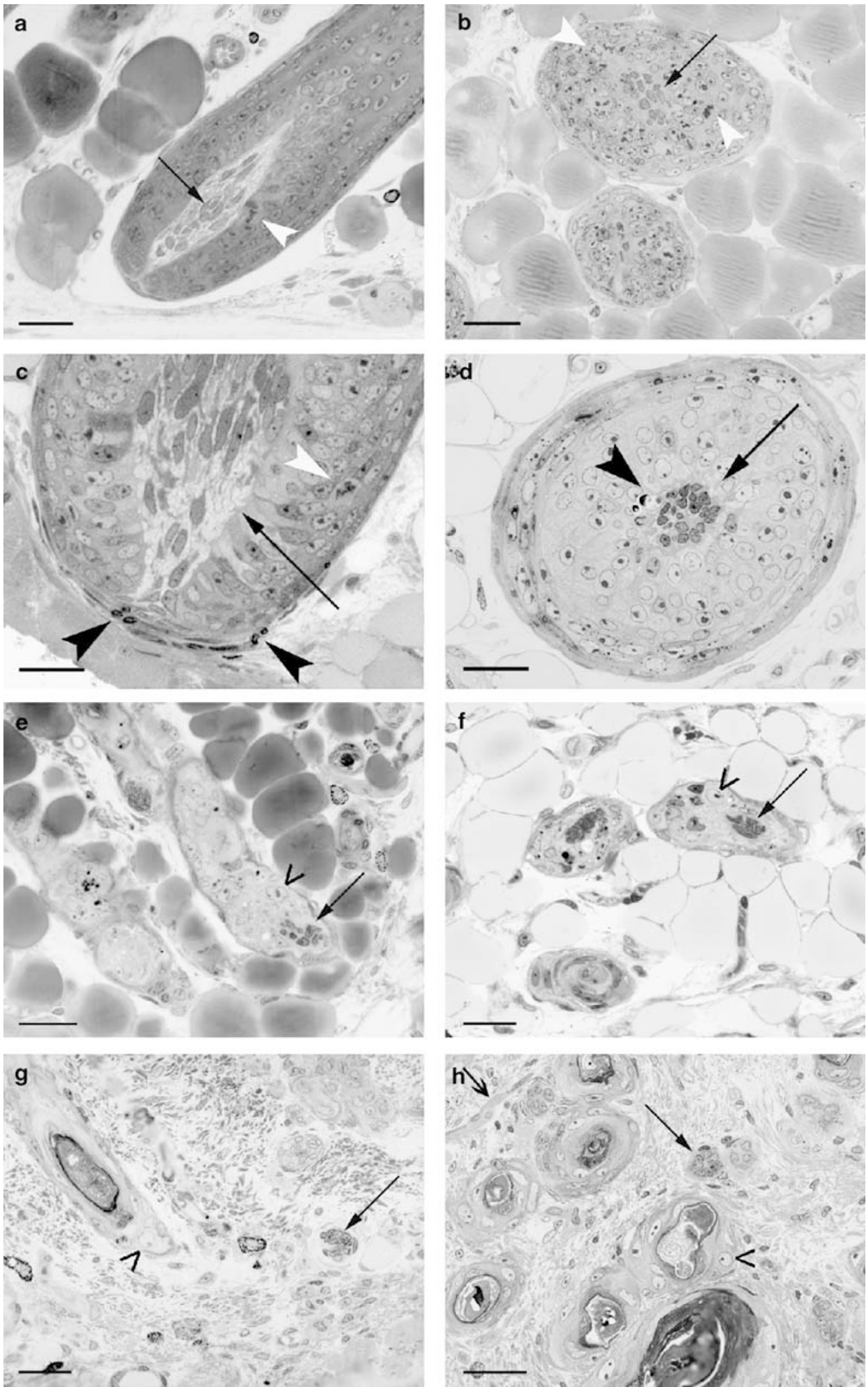

Figure 4 Longitudinal (left column) and transversal (right column) semithin sections of HFs from treated animals at T1 (**a**, **b**), T5 (**c**, **d**), T7 (**e**, **f**) and T10 (**g**, **h**). Arrows indicate the FP. Note the progressive reorientation of fibroblasts and the changes in the relationship between the FP and the HF. White arrow heads: mitosis. Black arrow heads: apoptosis. Note apoptotic cells in the CTS and in the matrix, close to the FP, at T5. Empty arrow heads: oncotic cells. The thin arrow in the upper left corner in (**h**) indicates a pilo-erector muscle. Bar: 30 μm.

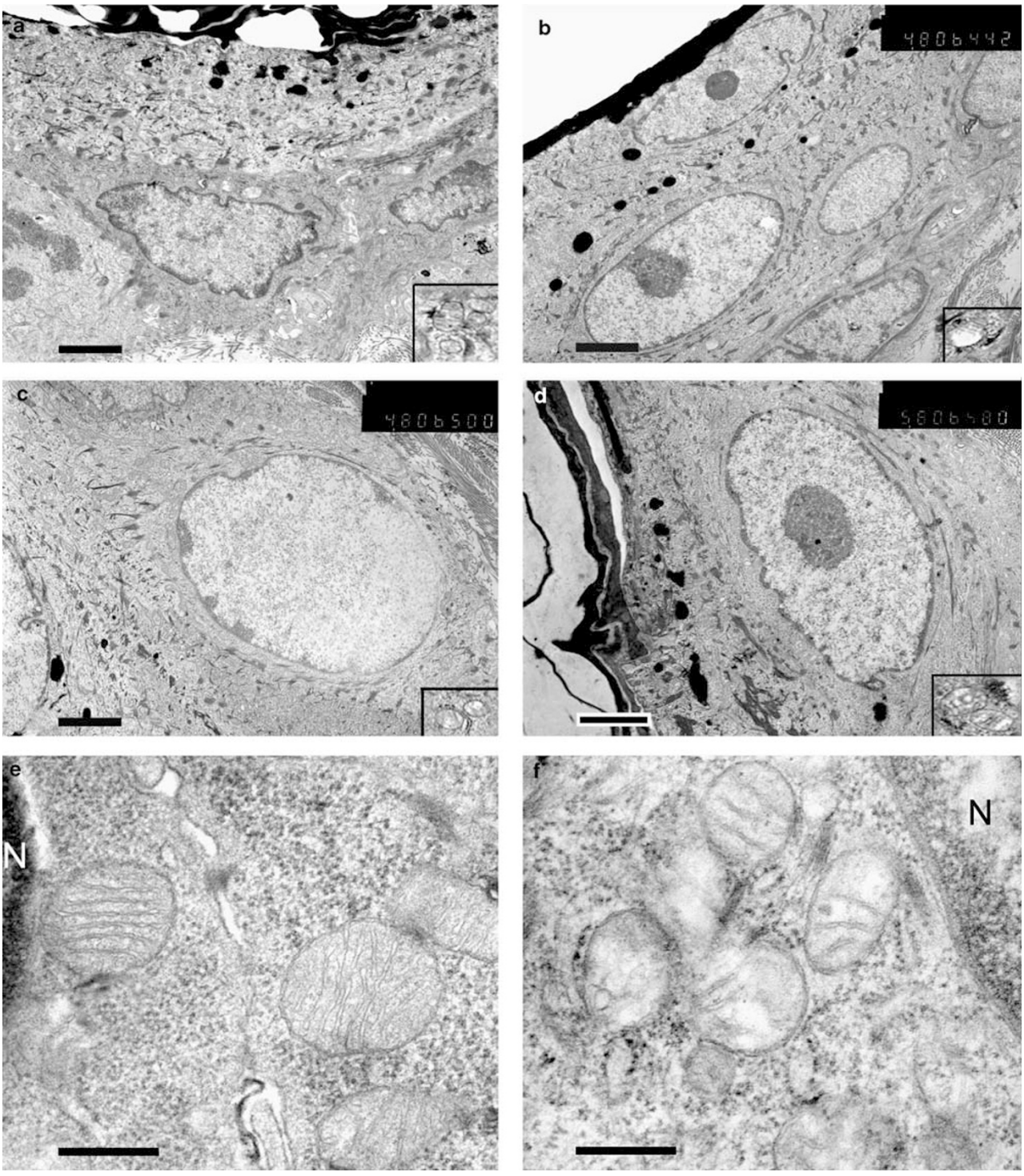

Figure 5 Electron microscopy of the epidermis from treated rats at T1 (**a**), T5 (**b**), T7 (**c**) and T10 (**d**). Inset: mitochondria, higher magnification. Note the increase in cristae damage with respect to time, and the progressive swelling and loss of convolute edges and chromatin rarefaction. Bar: 2 μm. (**e**) Higher magnification of the mitochondria at T1. Note the correct organization of membranes. Bar: 500 nm. (**f**) higher magnification of the mitochondria at T5. Note the loss of cristae organization, but the maintenance of the external double membrane, indicating that changes in membranes are not imputable to artifacts occurred during sample processing. N: nucleus. Bar: 500 nm.

keratinocytes showed oncotic features, but in this case, these features were observed in only a small percentage, approximately 2.69%, of the keratinocytes (Tables 1 and 2; Figures 7b and 8).

Observations by electron microscopy confirmed that epidermal cell shape in treated animals was more regular than that observed in control animals. Nuclei of epidermal cells were often enlarged with

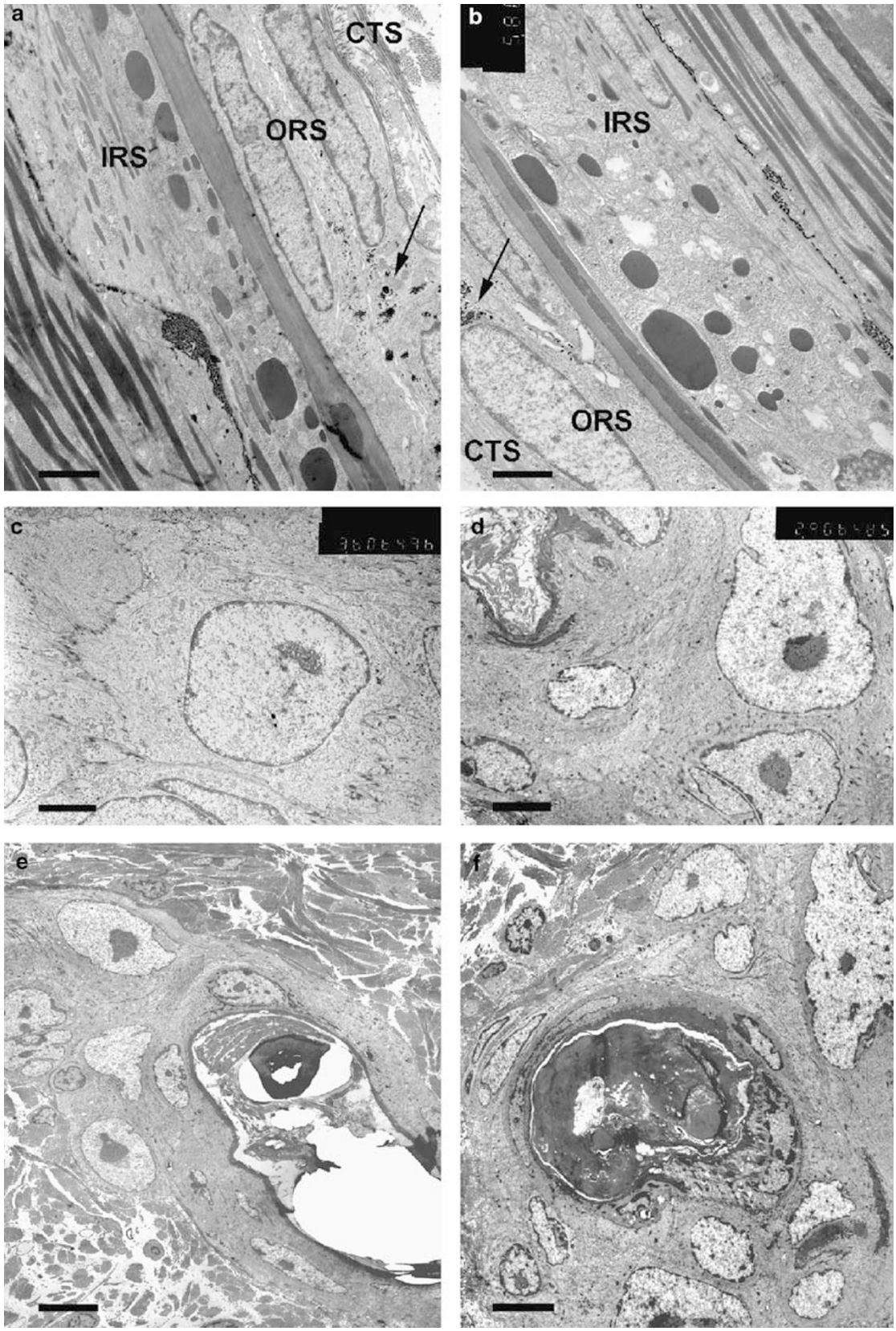

Figure 6 Electron microscopy of samples from treated animals at T1 (**a**), T5 (**b**), T7 (**e**), T10 (**f–h**). (**a**, **b**) Longitudinal sections; (**c–f**): transversal sections, showing oncotic ORS cells. Arrow indicates glycogen granules. In (**e**, **f**), note the collapse of the hair structure into the pilary canal. Bars: (**a**) 1.8 μm; (**b**) 2 μm; (**c**) 2.5 μm; (**d**) 3 μm; (**e**) 10 μm; (**f**) 4 μm.

Table 1 Number of apoptotic cells, mitoses and oncotic cells, expressed as the percentage of the total number of cells

	Hair follicle							*Epidermis*		
	ORS			*Matrix*		*CTS*		*Apoptosis*	*Mitosis*	*Oncosis*
	Apoptosis	*Mitosis*	*Oncosis*	*Apoptosis*	*Mitosis*	*Apoptosis*	*Mitosis*			
Control	0.22±*0.15*	0.55±*0.26*			2.07±*0.39*					0.63±*0.29*
T1		0.25±*0.17*	0.10±*0.10*		1.51±*0.34*			0.10±*0.10*		1.44±*0.47*
T5	0.47±*0.33*	0.10±*0.10*	2.69±*1.22*	3.16±*0.97*	1.00±*0.54*	20.10±*4.43*				18.60±*3.45*
T7	1.9±*0.76*		26.04±*2.63*	2.87±*1.04*	1.67±*0.90*	12.22±*4.29*				39.53±*2.19*
T10	0.75±*0.75*		75.64±*3.11*							70.63±*2.71*

Mean values and relevant±*standard errors* are quoted. Zero-values have been omitted. All data have been subjected to univariate variance analysis, using a fully factorial model. All source of errors (treatment and site) were significant ($P<0.01$) for all the observed cellular aspects (apoptosis, mitosis, oncosis). Since interaction site × treatment was also significant, it was decided to analyze the three sites separately. In both the ORS and the epidermis, the only cellular aspect that differs significantly between treatments is oncosis. Within the bulb, only the percentage of apoptotic cells differs significantly. In all cases that presented statistical differences, a *post hoc* Scheffé test has been carried out (see Table 2).

Table 2 Variance analysis by a *post hoc* Scheffé test based on the values reported in Table 1

Epidermis—oncotic cells

Treatment schedule	*Subset*			
	1	*2*	*3*	*4*
Control	0.6314			
T1	1.4422			
T5		18.6016		
T7			39.5293	
T10				70.6317

ORS—oncotic cells

Treatment schedule	*Subset*		
	1	*2*	*3*
Control	0.0000		
T1	0.0980		
T5	2.6939		
T7		26.0439	
T10			75.6415

Matrix—apoptotic cells

Treatment schedule	*Subset*	
	1	*2*
Control	0.0000	
T1	0.0000	
T7		2.8669
T5		3.1626

CTS—apoptotic cells

Treatment schedule	*Subset*	
	1	*2*
Control	0.0000	
T1	0.0000	
T7		12.2222
T5		20.1010

Mean values for homogeneous subsets are quoted (increasing order). In subsets collected together, treatment groups are not significantly different, while different subsets are significantly different (alpha = 0.5).

chromatin condensed at the nuclear edge, while the remaining nuclear content appeared to be less dense and a big nucleolus was also evident in either the centre or at the periphery of the nucleus (Figure 5b). Furthermore, although mitochondria were present with an intact outer membrane, a loss of the correct organization of the cristae was sometimes evidenced, suggesting that cristae damage could not be imputed to processing artifacts (Figures 5e, f).

In the hair follicle, ORS cells showed a reduction in glycogen content and mitochondria often appeared swollen and with damaged cristae. IRS, cortex and medulla cells were normal (Figure 6b).

T7 Oncosis is Detected in the ORS

At the T7 time point, control animals failed to display any characteristic difference with respect to the other time points. In treated animals, light microscopy revealed that 39.5% of epidermal keratinocytes were oncotic (Figure 2c; Tables 1 and 2; Figures 7a and 8). In the hair follicle, the initial phases of follicular structure degeneration were observed (Figure 4e, f). In total, 26% of ORS keratinocytes displayed oncosis (Tables 1 and 2; Figures 7b and 8). Cells within the matrix showed rare apoptotic figures (Tables 1 and 2; Figures 7c and 9). The FP appeared to lose its close relationship to the bulb, even though the FP was still surrounded

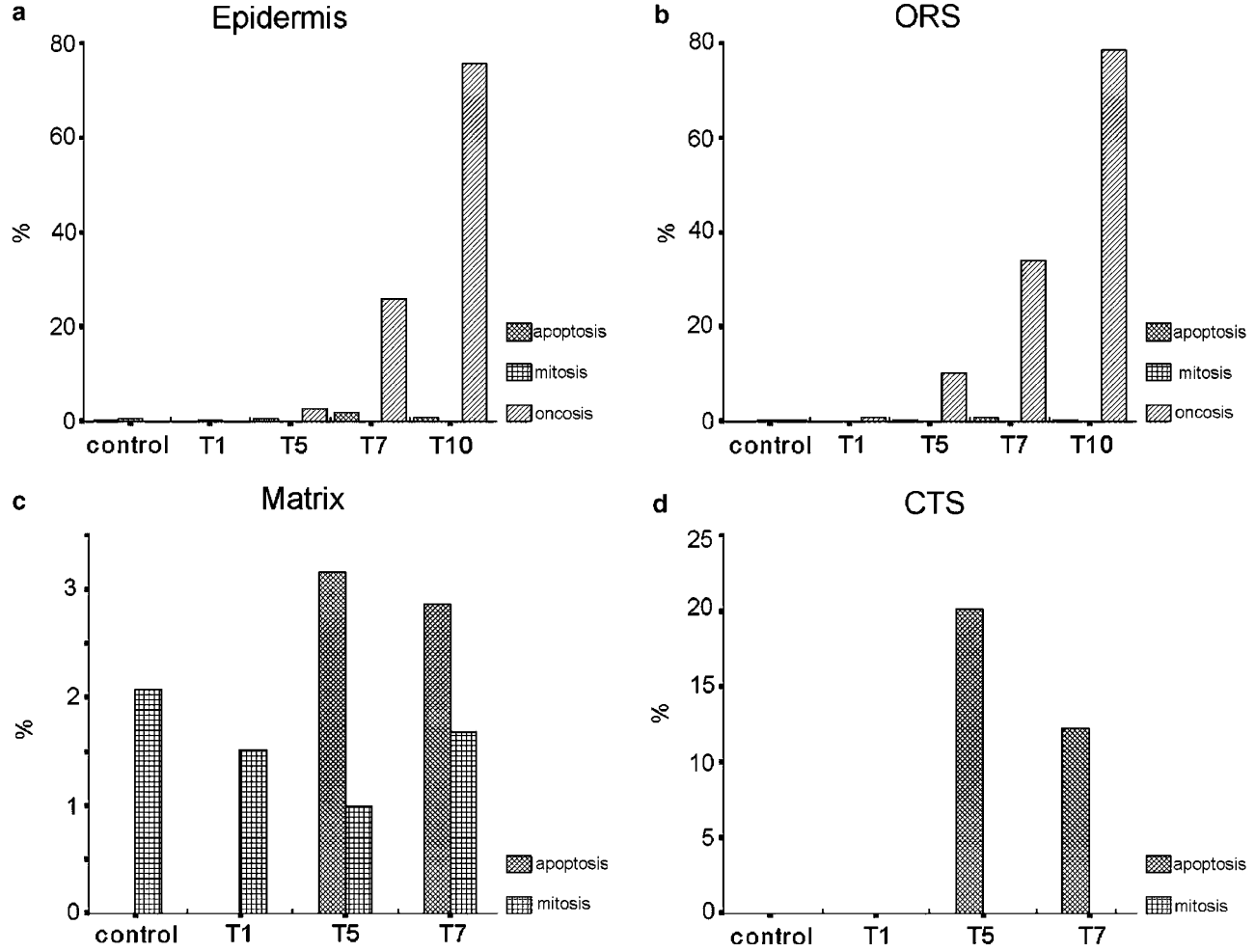

Figure 7 Graphical representation of the distribution of apoptosis, mitosis and oncosis in epidermis (**a**), ORS (**b**), matrix (**c**) and CTS (**d**) at different time points.

by bulbar cells in some hairs (Figure 4e). CTS fibroblasts showed apoptotic forms that were directly comparable to the ones formerly documented in the previous time point (Tables 1 and 2; Figures 7d and 9). At this time point, we also noted a reduction of the panniculum adiposum, that was still present (Figure 4e), but disposed prevalently within the deep portions of dermis.

Under electron microscopy, epidermal keratinocytes appeared more rounded in shape with respect to control cells. General cell dimension also increased. Nuclei were larger than normal and revealed a preferential distribution of chromatin to the edges of the nucleus (Figure 5c).

Within the hair follicle, both nuclei and ORS cells seemed swollen and their mitochondria were damaged. Glycogen granules were not detectable. The rough endoplasmic reticulum was preserved but the number of free cytoplasmic ribosomes diminished with respect to the control thus making the cytoplasm appear generally more dispersed (Figure 6c). These features all clearly suggested *an* oncotic process.

T10: An Increase in Oncosis within the Epidermis and ORS, and Movement of the HF towards the Epidermis—the Terminal Stage of the HF-Regressing Pathway

At T10, control animals continued to show no particular differences with respect to the control animals of other time points during the experiment. Treated animals displayed alopecia in the occipital region (over the head and the proximal part of the neck).

Analysis of the epidermis revealed a larger number of oncotic cells with respect to T7 (Tables 1 and 2 and Figures 7a and 8), and its surface appeared rough (Figure 2d).

HFs degenerated and profound morphological changes involving the entire three-dimensional architecture were observed. These changes were similar to a dystrophic catagen stage. The follicle assumed a screw-like shape and decreased in size and the shaft appeared to collapse within the pilary canal. The typical ordered structure of medulla, cortex and cuticle was lost, consequently becoming shrunken, small and spiraled (Figure 10). Alkaline

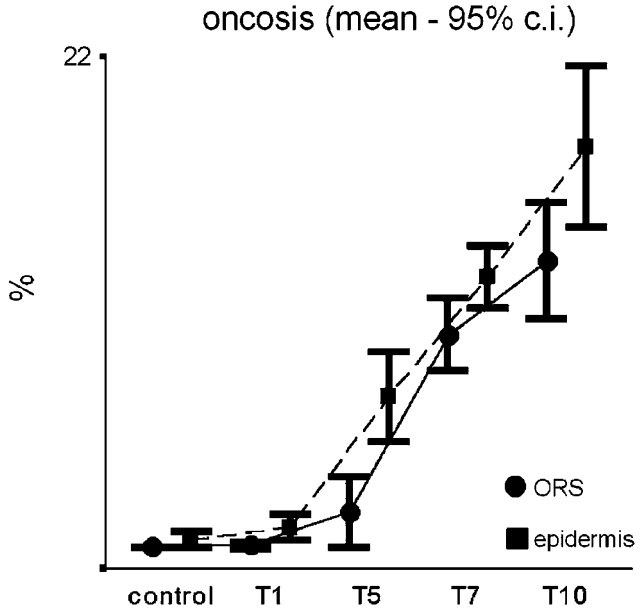

Figure 8 Graphical representation of the mean values and 95% confidence intervals of oncosis in the epidermis and the ORS at different time points. See Materials and methods section for the parameters used to distinguish between normal and oncotic cells.

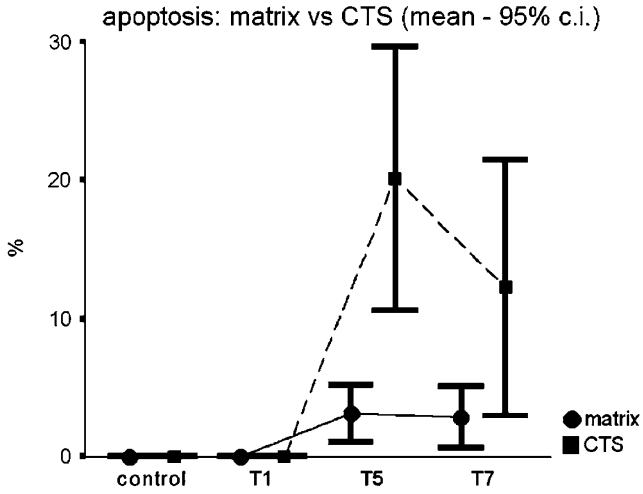

Figure 9 Graphical representation of the mean values and 95% confidence intervals of apoptosis in the matrix and the CTS at different time points.

phosphatase staining indicated that the follicle moved away from the FP, but it was still connected to it by an epithelial strand (Figure 11). Fibroblasts of the FP were condensed into a ball-like cluster, indicating the quiescent state of the cells. No apoptosis was detected. In untreated animals, the FP was lodged within the bulb, thus paralleling the observations of a normal anagen phase. Mitotic forms were observed within the matrix (data not shown). Oncotic cells of the ORS from treated animals accounted for 75.64% of the total number of ORS keratinocytes (Figures 4g, h and 10 and

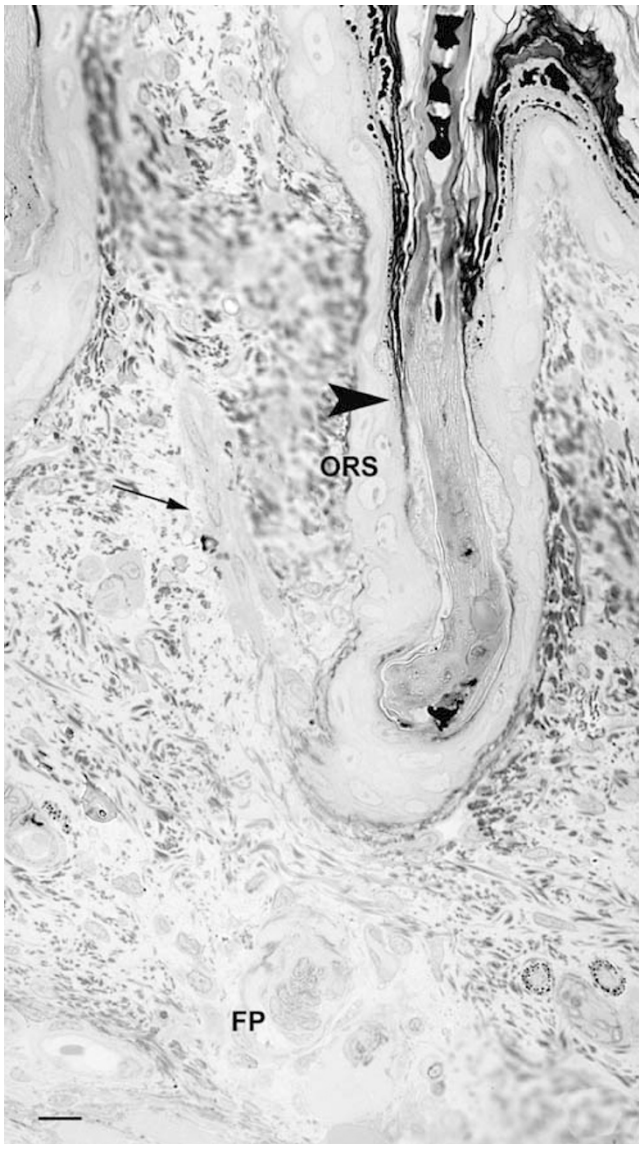

Figure 10 Semithin longitudinal section of an HF at T10. Note the condensation of the FP and the rise of the follicle toward the epidermis, the oncotic features of ORS cells, the degeneration of the IRS and the hair in the pilary canal. Arrow: pilo-erector muscle. Arrow head: IRS. Bar: 10 μm.

Tables 1 and 2). Alopecia was further accompanied by the sudden loss of the transitory portion of the hair.

Fat cells, which were large and numerous in controls, progressively regressed in treated rats. In fact, these cells were very small and had almost totally disappeared in animals showing alopecia. This is in accordance with the observed loss of animal body weight, which was clearly noticed during treatment. Adipocytes did not show apoptotic or oncotic features: the decrease in size of the panniculum adiposum is probably only due to a decrease in lipidic content of cells after the metabolic stress induced by drug administration.

A progressive reduction in number of blood vessel in the dermis was also observed.

Electron microscopy confirmed that keratinocytes from treated epidermis were swollen, contained large nuclei in which a large nucleolus was present, and with chromatin selectively condensed to the nuclear edges. Cells displayed a more dispersed cytoplasm with respect to what was observed for control cells, probably due to the fewer number of keratin bundles, and mitochondria appeared damaged (Figure 5d).

In the HF, ORS cells showed a major reduction of glycogen granules to the point where they nearly disappeared completely (Figure 6d–f). As observed in the epidermis, keratinocytes of the ORS also appeared swollen. In these abnormal cells, the mitochondria appeared swollen and the organization of the cristae was damaged. Since the same mitochondria also displayed an intact external double-membrane, we can exclude the occurrence of artifacts during sample processing. The cytoplasm showed regular numbers of keratin bundles and free ribosomes. The rough endoplasmic reticulum appeared large and evident membrane systems and vesicles were present (data not shown). As observed by light microscopy, the hair shaft appeared very condensed and the organization of the medulla was indistinguishable from that of the fiber. The shape of the fiber was not round in section, generally appeared collapsed and showed an abnormal aggregation of electron dense material (Figure 6e, f). Furthermore, the IRS appeared irregular, following the morphological alteration of the entire HF (Figure 6e, f).

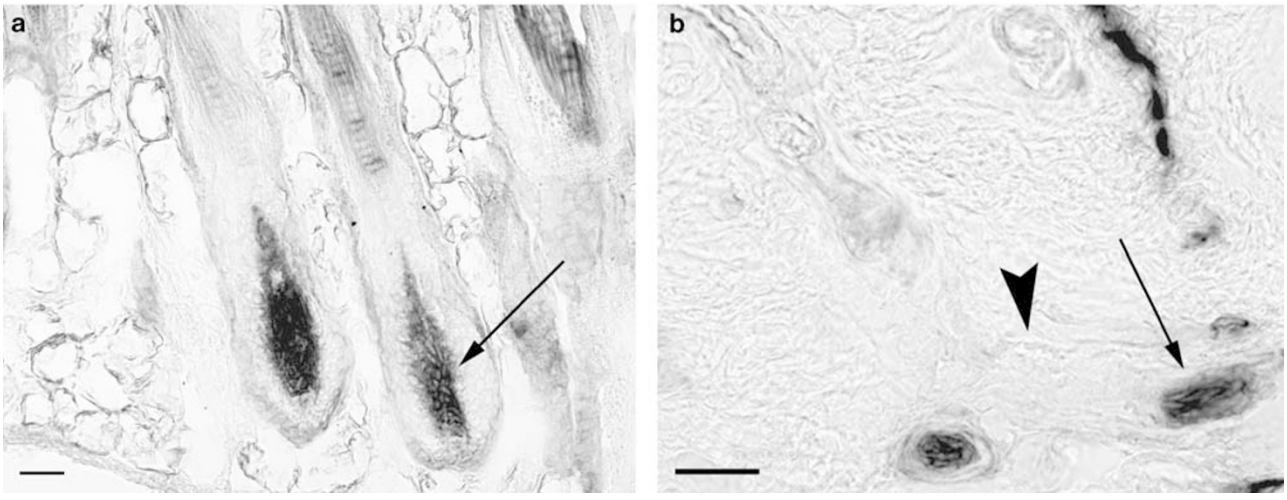

Figure 11 Cryosections of longitudinal HFs from treated animals at T1 (**a**) and T10 (**b**), stained for alkaline phosphatase. Arrow: FP; arrow head: epithelial strand. Note the condensation of the FP and the maintenance of contact with the upper follicle through the epithelial strand in T10. Other marked structures in (**b**) are vessels. Bar: 30 μm.

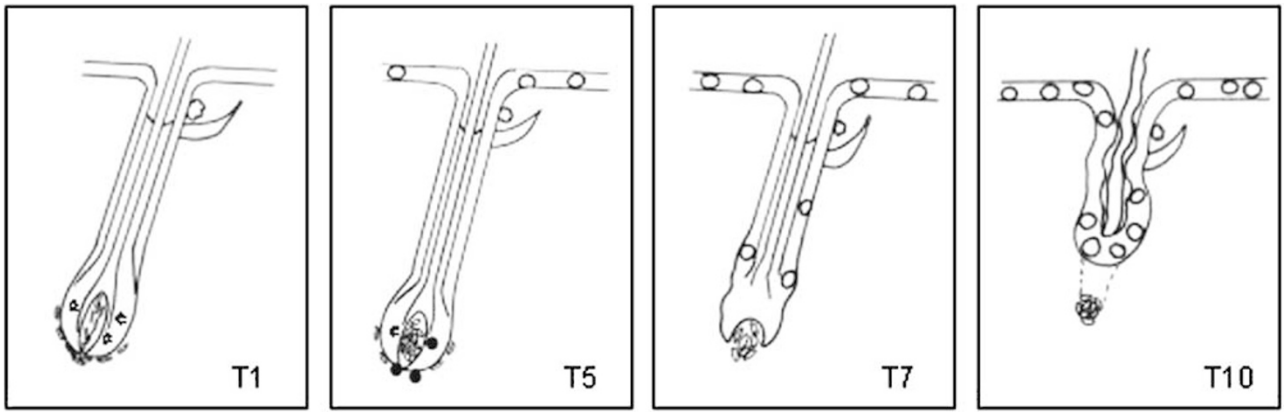

Figure 12 Schematic representation of the DXR-induced dystrophic catagen stage. T1 (1 day after the first DXR injection): in the matrix, about 2% of the cells were in mitosis. T5 (1 day after the last DXR injection): first significant signs of suffering in the epidermis. About 19% of keratinocytes are oncotic. Apoptosis, occasionally detected in the matrix compartment, is more represented in the CTS. T7 (3 days after the last DXR injection): number of oncotic cells increase both in the epidermis and in the ORS. T10 (6 days after the last DXR injection): the HF appears to have completed is dystrophic catagen pathway and alopecia subsequently arises.

Discussion

This is the first comprehensive study of the modifications occurring in the mesenchymal and the epithelial compartments during the regression of the hair follicles induced by DXR treatment. In our model, we observed that hair follicle degeneration proceeded in distinct steps and in a precise sequence of events that involved both the mesenchymal and epithelial components of the hair follicle (Figure 12). Hair follicle degeneration arose rapidly 5 days after the initiation of DXR treatment and lead to hair loss by a 'dystrophic catagen' pathway. 'Dystrophic catagen' is a form of rapid response of the HF to chemotherapy-induced damage. As previously described by Paus *et al*[20] and Ohnemus *et al*[21] this stage is characterized by shortened, catagen-like HF and abnormally dilated hair canals that do not contain hair shafts. These characteristics are also associated to pigmentary abnormalities. Although we did not observe these exact symptoms, probably due to differences in both animal models (albino rats *vs* black mice) and chemotherapy treatment, the morphological changes observed, particularly occurring in T10, paralleled the characteristic features (eg rapid HF shortening) of the dystrophic catagen phenomenon (Figure 10).

Mesenchymal Compartment

The involvement of the mesenchymal compartment in both CTS and FP was detected in our experiments a single day after the end of treatment (T5).

With respect to the CTS, apoptotic fibroblasts were observed surrounding the lower portion of the bulb, near the opening that connects the FP to the CTS. Apoptosis is known to be involved in a wide number of remodeling phenomena, and frequently accompanies differentiative processes. During development and differentiation, organs and tissues are frequently sculpted through the addition or subtraction of cells, respectively by mitosis and programmed cell death.[22,23] The cycling portion of the hair follicle proceeds through repeated growth and regression events and thus, the involvement of mitosis and apoptosis in this processes are commonly accepted.[24] During physiological catagen, apoptosis in the epithelial cells of the transient portion of the follicle has been proposed as the pivotal mechanism involved in the reduction of cell number.[25,26] Some authors particularly emphasize that the involvement of apoptosis of the CTS can contract and squeeze or push the follicle towards the epidermis.[27–29] In our opinion, apoptosis that induces the retraction of the CTS may further provide a mechanical signal leading to the degeneration of the entire hair follicle and in particular, the more proximal matrix cells. In fact, several studies have reported the importance of mechanical stimuli to the induction of apoptosis.[30–32]

At T5, important modifications were also noted in the FP which is the second mesenchymal compartment of the hair follicle. FP cells, which originally aligned their major axis parallel to the direction of hair growth, were observed to randomize their orientation, thus losing their cylindrical organization within the bulb (this phenomenon is known in pathology as 'loss of polarity of cells'). These modifications lead to the reduction of contact surface between FP and matrix cells. Fibroblasts lost their homogeneous shape and began to both condense and reduce their biosynthetic activity, as suggested by the decrease in extracellular matrix (ECM). This has been reported to also occur in physiological catagen.[17] Due to the release of many morphogenetic factors, the FP has an important role in regulating the proliferation, differentiation and degeneration of matrix keratinocytes.[33,34] This activity requires that both matrix cells and fibroblasts maintain close contacts via the ECM.[34,35] Therefore, the involution of matrix cells may by assisted by the reduction of the physical relationships between FP cells and the matrix, the direct action of DXR and the mechanical stimuli arising from CTS retraction.

In our experiments, apoptosis in the FP was never detected. This agrees with previous data reported on physiological catagen,[26] which confirmed the FP as a protected site, probably due to expression of antiapoptotic molecules such as BCL-2.[24,36]

Moreover, we noted the presence of an epithelial strand that maintained the FP connected to the follicle (see Figure 11). During physiological catagen, it is known that this epithelial strand plays a pivotal role in the regrowth of a new HF by guiding stem cells towards the FP.[37] We speculate that in chemotherapy-induced alopecia, the close relationship between the FP and this epithelial strand plays a similar pivotal role in guaranteeing the growth of a new follicle, thus rendering hair loss reversible.

Epithelial Compartment

It has been proposed that apoptosis in matrix cells is the major cause of chemotherapy induced hair loss.[9,38] However, in our experimental model of DXR-induced alopecia, we observed only a low number of apoptotic forms in the matrix. The apoptosis might be related to a DXR-induced down-regulation of beta-catenin expression;[39] this protein has been reported to play an antiapoptotic role on matrix cells.[40] The lack of a great number of apoptotic cells suggested that apoptosis may not be the only form of cellular damage within the epithelial compartment of DXR-treated hair follicles. Accordingly, Cece *et al*[10] reported only a minimal number of apoptotic cells in the bulb of hairs of DXR treated animals (maximum 1.2%). It is possible that the differences reported in literature may depend on either the animal model or the drug type and schedule used (acute or chronic treatments). In

order to better parallel the protocols used in the clinic, low drug doses, compatible with prolonged treatments, were adopted for our animal model. This is in contrast to the acute treatments that are normally used with animals in similar studies.[20] It is noteworthy that in the tongue epithelium of mice treated with DXR, apoptosis was observed only after the administration of high drug doses.[41]

In order to explain the regression that occurs in the epithelial compartment in the absence of high levels of apoptosis, another mechanism of cell deletion must play a role. We observed that keratinocytes in the epidermis at T5, and in both the epidermis and the ORS at T7, underwent morphological changes leading to swollen nuclei with chromatin condensed to the nuclei edges, a big nucleolus and dispersed cytoplasm. These changes became much more evident in the subsequent time point (T10). We identify these morphologically different cells as oncotic. Oncosis is described as a form of cell death, which is distinct from apoptosis, even though some steps leading to cell death are shared between these two mechanism.[42,43] As reported above, oncosis is due to the failure of ionic pumps on the plasma membrane, and is typically caused by ischemia and toxic agents that interfere with ATP generation or increase membrane permeability.[13] DXR is known to both damage ionic pumps on the plasma membrane and to interfere with mitochondrial activity.[44–46] Moreover, DXR has been also reported to induce oncosis in different cells types, such as human endothelial cells,[15] melanoma[47] and myocytes.[48]

Depletion of the glycogen content in ORS cells, which was clearly evident in our samples from T7 (data not shown) and T10, has been reported as one of the side effects of DXR.[49,50] Glycogen metabolism is very important in the epidermis and, in particular, within the hair follicle.[37] In general, the accumulation of glycogen granules is inversely proportional to metabolic activity.[17] Data reported in literature have suggested that glucose transport may represent an early target for DXR.[51] It is thus possible to suggest that ORS cells tend to accelerate their activity in order to face the metabolic stresses caused by increasing DXR-induced damage, but the extensive injuries caused prevent the formation of new granules. The reduction in the amount of glycogen in ORS cells may therefore explain the high level of oncosis.

Taken together, our data suggest the need to re-evaluate the role of the mesenchymal compartment of the hair follicle in chemotherapy-induced alopecia, and more generally, in hair-remodeling processes. We further demonstrate the role of an alternative cell death mechanism, namely oncosis, responsible for hair regression in chemotherapy-induced alopecia. Further studies addressing the molecular pathway of oncosis could be useful in providing the framework for new therapies directed at preventing chemotherapy-induced alopecia.

Acknowledgement

This work was partially supported by a grant from AIRC.

References

1 Crounse RG, Van Scott EJ. Changes in scalp hair roots as a measure of toxicity from cancer chemotherapeutic drugs. J Dermatol Invest 1960;35:83–90.
2 Howser DM. Alopecia—the problem of alopecia in cancer. In: Groenwald SL, Frogge MH, Goodman M (eds). Cancer Symptom Management. Jones and Bartlett: Boston, MA, 1996, pp 261–268.
3 Moseley J. Nursing management of toxicities associated with chemotherapy for lung cancer. Semin Oncol Nurs 1987;3:202–210.
4 Junqueira LC, Carneiro J, Kelly RO. Subcutaneous tissue—hairs. In: Appleton (ed). Basic Histology, 8th edn. Lange Medical Books: Stanford, CT, 1995, pp 352–355.
5 Batchelor D. Hair and cancer chemotherapy: consequences and nursing care—a literature study. Eur J Cancer Care 2001;10:147–163.
6 Didonato K. Standards of clinical nursing practice: alopecia. Cancer Nurs 1985;8:76–77.
7 Cline BW. Prevention of chemotherapy-induced alopecia: a review of the literature. Cancer Nurs 1984;7:221–228.
8 Goldberg MT, Tackaberry LE, Hardy MH, *et al.* Nuclear aberrations in hair follicle cells of patients receiving cyclophosphamide. Arch Toxicol 1990;64:116–121.
9 Botchkarev VA, Komarova EA, Siebenhaar F, *et al.* p53 is essential for chemotherapy-induced hair loss. Cancer Res 2000;60:5002–5006.
10 Cece R, Cazzaniga S, Morelli D, *et al.* Apoptosis of hair follicle cells during doxorubicin-induced alopecia in rats. Lab Invest 1996;75:601–609.
11 Tobin DJ, Gunin A, Magerl M, *et al.* Plasticity and cytokinetic dynamics of the hair follicle mesenchyme during the hair growth cycle: implications for growth control and hair follicle transformations. J Invest Dermatol Symp Proc 2003;8:80–86.
12 Hussein AM, Jimenez JJ, McCall CA, *et al.* Protection from chemotherapy-induced alopecia in a rat model. Science 1990;249:1564–1566.
13 Majno G, Joris I. Apoptosis, oncosis, and necrosis. An overview of cell death. Am J Pathol 1995;146:3–15.
14 Romashko J, Horowitz S, Franek WR, *et al.* MAPK pathways mediate hyperoxia-induced oncotic cell death in lung epithelial cells. Free Radic Biol Med 2003;35:978–993.
15 Mailloux A, Grenet K, Bruneel A, *et al.* Anticancer drugs induce necrosis of human endothelial cells involving both oncosis and apoptosis. Eur J Cell Biol 2001;80:442–449.
16 Mills EM, Xu D, Fergusson MM, *et al.* Regulation of cellular oncosis by uncoupling protein 2. J Biol Chem 2002;277:27385–27392.
17 Montagna W, Parakkal PF. The Structure and Function of Skin, 3th edn. Academic Press: New York, 1974.
18 Snedecor GW, Cochran WG. Statistical Methods. Iowa State University Press: Ames, IA, 1972.
19 Armitage P. Statistical methods in medical research. Blackwell Scientific: Oxford, 1973.

20 Paus R, Handjiski B, Eichmuller S, *et al.* Chemotherapy-induced alopecia in mice. Induction by cyclophosphamide, inhibition by cyclosporine A, and modulation by dexamethasone. Am J Pathol 1994; 144:719–734.
21 Ohnemus U, Űnalan M, Handjiski B, *et al.* Topical estrogen accelerates hair regrowth in mice after chemotherapy-induced alopecia by favoring the dystrophic catagen response pathway to damage. J Invest Dermatol 2004;122:7–13.
22 White E. Life, death and the pursuit of apoptosis. Genes Dev 1996;10:1–15.
23 Gilbert SF. Developmental Biology, 5th edn. Sinauer: Sutherland, MA, 1997, pp 543–590, 883–918.
24 Stenn KS, Paus R. Controls of hair follicle cycling. Physiol Rev 2001;81:449–494.
25 Weedon D, Strutton G. Apoptosis as the mechanism of the involution of hair follicles in catagen transformation. Acta Dermatol Venereol 1981;61:335–369.
26 Lindner G, Botchkarev VA, Botchkareva NV, *et al.* Analysis of apoptosis during hair follicle regression (catagen). Am J Pathol 1997;151:1601–1617.
27 Ito M, Sato Y. Dynamic ultrastructural changes of the connective tissue sheath of human hair follicles during hair cycle. Arch Dermatol Res 1990;282:434–441.
28 Reynolds AJ, Chaponnier C, Jahoda CA, *et al.* A quantitative study of the differential expression of alpha-smooth muscle actin in cell populations of follicular and non-follicular origin. J Invest Dermatol 1993;101:577–583.
29 Metze D, Theissen U, Zelger B, *et al.* Myofibroblasts are a regular component of the fibrous sheath of human hair follicles. Br J Dermatol 1994;131:179.
30 Wernig F, Xu Q. Mechanical stress-induced apoptosis in the cardiovascular system. Prog Biophys Mol Biol 2002;78:105–137.
31 Gupta R, Steward O. Chronic nerve compression induces concurrent apoptosis and proliferation of Schwann cells. J Comp Neurol 2003;461:174–186.
32 Weyts FA, Bosmans B, Niesing R, *et al.* Mechanical control of human osteoblast apoptosis and proliferation in relation to differentiation. Calcif Tissue Int 2003;72:505–512.
33 Link RE, Paus R, Stenn KS, *et al.* Epithelial growth by rat vibrissae follicles *in vitro* requires mesenchymal contact via native extracellular matrix. J Invest Dermatol 1990;95:202–207.
34 Jahoda CA, Reynolds AJ. Dermal–epidermal interactions. Adult follicle-derived cell populations and hair growth. Dermatol Clin 1996;14:573–583 (review).
35 Tian B, Lessan K, Kahm J, *et al.* beta 1 integrin regulates fibroblast viability during collagen matrix contraction through a phosphatidylinositol 3-kinase/Akt/protein kinase B signaling pathway. J Biol Chem 2002;277:24667–24675.
36 Sellheyer K, Krahl D, Ratech H. Distribution of Bcl-2 and Bax in embryonic and fetal human skin: anti-apoptotic and proapoptotic proteins are differentially expressed in developing skin. Am J Dermatopathol 2001;23:1–7.
37 Williams R, Philpott MP, Kealey T. Metabolism of freshly isolated human hair follicles capable of hair elongation: a glutaminolytic, aerobic glycolytic tissue. J Invest Dermatol 1993;100:834–840.
38 Botchkarev VA. Molecular mechanisms of chemotherapy-induced hair loss. J Invest Dermatol Symp Proc 2003;8:72–75.
39 Sadot E, Geiger B, Oren M, *et al.* Down-regulation of beta-catenin by activated p53. Mol Cell Biol 2001;21:6768–6781.
40 Hassanein AM, Glanz SM. Beta-catenin expression in benign and malignant pilomatrix neoplasms. Br J Dermatol 2004;150:511–516.
41 Balsari A, Rumio C, Morelli D, *et al.* Topical administration of a doxorubicin-specific monoclonal antibody prevents drug-induced mouth apoptosis in mice. Br J Cancer 2001;85:1964–1967.
42 Lecoeur H, Prevost MC, Gougeon ML. Oncosis is associated with exposure of phosphatidylserine residues on the outside layer of the plasma membrane: a reconsideration of the specificity of the annexin V/propidium iodide assay. Cytometry 2001;44:65–72.
43 Jaeschke H, Lemasters JJ. Apoptosis versus oncotic necrosis in hepatic ischemia/reperfusion injury. Gastroenterology 2003;125:1246–1257.
44 Eckenhoff RG, Somlyo AP. Cardiac mitochondrial calcium content during fatal doxorubicin toxicity. Toxicol Appl Pharmacol 1989;97:167–172.
45 Iwasaki T, Suzuki T. Ultrastructural alterations of the myocardium induced by doxorubicin. A scanning electron microscopic study. Virchows Arch B Cell Pathol Incl Mol Pathol 1991;60:35–39.
46 Tritton TR. Cell surface actions of adriamycin. Pharmacol Ther 1991;49:293–309 (review).
47 Kuwashima Y. Cytomorphology of murine B16 melanoma in vivo after treatment with cyclophosphamide: evidence of 'oncotic' cell death. Anticancer Res 1996;16:2997–3000.
48 L'Ecuyer TJ, Allebban Z, Thomas R, *et al.* Glutathione-*S*-transferase overexpression protects against anthracycline-induced H9C2 cell death. Am J Physiol Heart Circ Physiol (Epub), Jan 15, 2004.
49 Vaudaux P, Kiefer B, Forni M, *et al.* Adriamycin impairs phagocytic function and induces morphologic alterations in human neutrophils. Cancer 1984;54: 400–410.
50 Gabizon A, Meshorer A, Barenholz Y. Comparative long-term study of the toxicities of free and liposome-associated doxorubicin in mice after intravenous administration. J Natl Cancer Inst 1986;77:459–469.
51 Hrelia S, Fiorentini D, Maraldi T, *et al.* Doxorubicin induces early lipid peroxidation associated with changes in glucose transport in cultured cardiomyocytes. Biochim Biophys Acta 2002;1567:150–156.